IN-24

171957

P13

NASA Technical Memorandum 106136

# Ceramic Matrix Composites Properties/ Microstresses With Complete and Partial Interphase Bond

Subodh K. Mital
*University of Toledo*
*Toledo, Ohio*

and

P.L.N. Murthy and C.C. Chamis
*Lewis Research Center*
*Cleveland, Ohio*

Prepared for the
38th International SAMPE Symposium/Exhibition
Anaheim, California, May 10–13, 1993

(NASA-TM-106136) CERAMIC MATRIX COMPOSITES PROPERTIES/MICROSTRESSES WITH COMPLETE AND PARTIAL INTERPHASE BOND (NASA) 13 p

N93-29071

Unclas

G3/24 0171959

NASA

# CERAMIC MATRIX COMPOSITES PROPERTIES/MICROSTRESSES WITH COMPLETE AND PARTIAL INTERPHASE BOND

Subodh K. Mital
University of Toledo
Toledo, Ohio 43606

and

Pappu L.N. Murthy and Christos C. Chamis
National Aeronautics and Space Administration
Lewis Research Center
Cleveland, Ohio 44135

## SUMMARY

A multilevel substructuring technique which includes a unique fiber substructuring concept is used for the analysis of continuous fiber reinforced ceramic matrix composites. This technique has four levels of substructuring—from laminate to ply, to subply, and then to fiber. A stand-alone computer code CEMCAN (CEramic Matrix Composites ANalyzer), incorporating this technique and specifically for the simulation of ceramic matrix composites behavior, is currently under development at NASA Lewis Research Center in Cleveland, Ohio. The thermal and mechanical properties, along with the microstresses, for a SiC/RBSN (silicon carbide fiber and reaction bonded silicon nitride matrix) composite at different fiber volume ratios and varying degrees of interfacial bond around the fiber circumference are computed. Values predicted by CEMCAN computer code are shown to bound the experimentally measured values. Results also show that transverse tensile strength test can be a sensitive test method to assess interfacial conditions.

## INTRODUCTION

In-house research at NASA Lewis Research Center in Cleveland, Ohio over the past two decades has focussed on the mechanics of materials approach for composite micromechanics and has resulted in several computer codes for composite micromechanics and macromechanics. The primary intention of this research is to develop composite mechanics theories and analysis methods that range in scale from micromechanics to global structural analysis in one integrated code. The micromechanics theories are represented by simplified equations and have been corroborated by experimental results and three-dimensional finite element analyses (refs. 1 and 2). Among these codes are ICAN (Integrated Composite ANalyzer) (ref. 3) and METCAN (METal Matrix Composites ANalyzer) (ref. 4). The ICAN and METCAN computer codes were developed specifically for continuous fiber reinforced polymer matrix and metal matrix composites, respectively.

Currently, ceramic matrix composites (CMC) are being developed for high speed engine applications because of their increased strength, fracture toughness and creep resistance in demanding service environments. To analyze the behavior of these ceramic matrix composites, a unique and novel substructuring technique has been developed and is being incorporated into a stand-alone computer code CEMCAN (CEramic Matrix Composites ANalyzer). This technique has four levels of substructuring—from laminate to ply, to subply, and then to fiber. The fiber is substructured into several slices and the micromechanics equations are applied at the slice level. Although the basic philosophy can be applied to the analysis of any continuous fiber reinforced composite, the emphasis here is on the development of a computer code to specifically analyze and simulate aspects unique to ceramic matrix composites. The aspects of interest include varying degrees of interfacial bond around the fiber circumference and accounting for the fiber breaks and local matrix cracking which may lead to rapid degradation of interphase at higher temperatures due to oxidation. In addition, the multilevel substructuring technique used in CEMCAN can account for different fiber shapes and integrate the effect of all of these aspects on composite properties/response and, in turn, provide a greater detail in stress distribution.

The objective of the present paper is to briefly describe the multilevel substructuring concept used in the CEMCAN computer code, and to show some illustrative examples to demonstrate the versatility of the code.

## NOMENCLATURE

| | |
|---|---|
| E | Young's modulus |
| G | shear modulus |
| $\alpha$ | coefficient of thermal expansion |
| $\nu$ | Poisson's ratio |
| K | thermal conductivity |

Subscripts

| | |
|---|---|
| $\ell$ | slice |
| f | fiber |
| m | matrix |
| i | interphase properties |
| 1-1 | longitudinal direction (along the fiber) |
| 2-2 and 3-3 | directions transverse to the fiber |

## FIBER SUBSTRUCTURING AND MICROMECHANICS

Composite micromechanics equations are used to determine the equivalent elastic properties of a composite material in terms of the elastic properties of the constituent materials. The properties of interest are composite moduli, Poisson's ratios, thermal expansion coefficients, thermal conductivities, heat capacity, etc., and various composite strengths.

The micromechanics equations are derived for a representative volume element (RVE), sometimes referred to as a "unit cell," which is the smallest region over which the stresses and strains are assumed to be macroscopically uniform. The unit cell consists of fiber, matrix, and possibly an interphase treated as a separate constituent. The geometry of the unit cell depends upon the chosen array pattern for the fibers, e.g., square, hexagon or any other kind of repeating geometry. Equivalent properties for the unit cell or RVE are then derived based on the constituent properties using a mechanics of materials approach. This approach is based on certain assumptions, in addition to a chosen array pattern, such as : (a) all the constituents are subjected to same strain in the fiber direction in the case of a unidirectional composite, and (b) the same transverse stress is applied to all the constituents in the direction transverse to the fiber. These are standard assumptions used for the derivation of micromechanics equations, but they are not mathematically rigorous. A mathematically rigorous solution that ensures the displacement continuity across the fiber and matrix boundary can be obtained through the use of theory of elasticity.

The representative volume element used previously for ICAN consisted of two distinct regions A (matrix only) and B (fiber and matrix). The unit cell for METCAN may consist of three distinct regions A, B, and C (fig. 1). The region A consists of pure matrix, the region B may consist of matrix and interphase, and region C consists of fiber, matrix, and interphase. The interphase is treated here as a distinct region with distinct mechanical and thermal properties. Thus, it can represent a reaction zone formed due to the chemical reaction between fiber and matrix or a separate layer provided intentionally to prevent such a reaction. The different regions facilitate representation of nonuniformity in local stress distribution.

This approach has been taken one step further for the analysis of ceramic matrix composites. Although the same square fiber array pattern is assumed, unit cell is further subdivided into several slices. The equations of micromechanics are derived for slices, i.e., slice equivalent properties are computed based on the properties of the fiber, matrix, and interphase. The fiber substructuring and slice geometry is shown in figure 2. The derivations of the micromechanics will not be given here as it was provided in some detail in a previous reference (ref. 5). For example, if $k_f$, $k_m$, and $k_i$ are fiber, matrix, and interphase volume ratios respectively, then (fig. 2)

$$k_f = \frac{d_f}{s}; \quad k_m = 2\frac{d_m}{s}; \quad k_i = 2\frac{d_i}{s}$$

The equivalent longitudinal slice modulus is given by,

$$E_{\ell 11} = k_f\, E_{f11} + k_m\, E_{m11} + k_i\, E_{i11}$$

The transverse modulus in the 2-2 direction is given by,

$$E_{\ell 22} = \frac{E_{m22}\, E_{f22}\, E_{i22}}{k_m\, E_{f22}\, E_{i22} + k_i\, E_{f22}\, E_{m22} + k_f\, E_{m22}\, E_{i22}}$$

and the longitudinal thermal expansion coefficient is given by,

$$\alpha_{\ell 11} = \frac{k_m \alpha_{m11} E_{m11} + k_i \alpha_{i11} E_{i11} + k_f\, \alpha_{f11} E_{f11}}{E_{\ell 11}}$$

Similarly, other mechanical and thermal properties are expressed are in terms of the constituent properties. Once the equivalent slice properties are obtained, the equivalent properties of the unit cell or RVE are obtained by using the laminate theory in an analogous manner as one would obtain laminate properties from ply properties. It should also be mentioned that 2-2 or horizontal slicing is used to compute 1-1 and 2-2 slice properties, while 3-3 or vertical slicing is used to compute slice properties in the 3-3 direction.

## CEMCAN COMPUTER CODE

This fiber substructuring technique and the micromechanics equations have been programmed into a stand-alone computer code CEMCAN. Only a brief description of the code will be provided here, since more detailed description was provided in an earlier report (ref. 5).

The integration of the slice properties to obtain the equivalent properties of a unit cell or RVE is accomplished by using the classical laminate theory. If there is only one fiber through the ply thickness, then the ply equivalent properties are identical to the properties of the unit cell or the RVE. If there are a number of fibers through the thickness of a single ply, then the unit cell properties have to be integrated by using the laminate theories again to obtain the ply properties. Then, the laminate or composite properties are obtained from the single ply properties by using macromechanics theories. The laminate theory will not be explained here as it can be found in any composite mechanics textbook (ref. 6, for example). After the laminate properties are computed, the next step is to obtain the laminate response due to externally applied loads. CEMCAN flowchart is shown in figure 3. The left side of the chart shows the composition or synthesis of the properties from slice to laminate level. The right hand side of the flowchart shows the decomposition of the response from laminate to ply, to slices, and then to microstresses.

CEMCAN computer code has a similar type of resident data bank as in the previously developed composite mechanics codes at NASA Lewis. The user needs to specify only the code names of the constituent materials in the input file and the program searches and selects the appropriate material properties from the data base. New materials can be easily added to the data base as they become available.

Currently, the code can predict the composite mechanical and thermal properties and can compute the stresses based on a linear laminate analysis. The stresses at ply, slice, or constituent levels can be obtained. The user can specify the number of slices in a unit cell and the state of interfacial bonding around the fiber circumference in each slice ranging from 0 (completely debonded) to 1 (fully bonded). To obtain the mechanical properties of the interphase, the values provided in the resident data bank will be multiplied by the factor (0 to 1) representing interfacial bonding. Thus, if the interphase in a slice is completely debonded, the mechanical properties of the interphase will be reduced to negligible (almost zero) values. As mentioned earlier, the code can currently carry out a linear laminate analysis only. Future modifications to the code will include capability to perform nonlinear laminate analysis, where the nonlinearity in the material behavior will be considered at the constituent level.

The CEMCAN, in conjunction with a finite element analysis code, can also be used to analyze woven composite materials. A typical element of the finite element model is shown in figure 4. Material properties at the nodes of the finite element model can be used for the analysis. Such properties, integrated through the thickness can be obtained by using CEMCAN at every node. For example, if a section is taken at A-A or B-B (fig. 4), there will be a certain number of 0 plies, certain number of cross-plies and matrix rich area. Each ply is represented by a unit cell (fig. 3) with proper orientation. The code will compute the ply properties and then integrate them through the thickness to obtain the nodal properties like force-deformation relations. The force-deformation relations at the nodes can then be used as input to the finite element model to analyze the structural component made from woven fabric material.

## RESULTS/DISCUSSION

The composite system analyzed here is a unidirectional SiC/RBSN (silicon carbide SCS–6 fibers in reaction bonded silicon nitride matrix). The thickness of the interphase is taken as 5 percent of the fiber diameter. The typical properties of these constituents based upon the data given in reference 7 are listed in table I. In computing the composite properties and the response, both a strong and a weak interphase have been considered. In a strong interphase, the properties of the interphase are taken to be the same as the matrix properties, while in the case of a weak interphase, the normal and shear moduli of the interphase are reduced to negligible (near zero) values. Thus, the lower and upper bounds to the mechanical properties can be established. The fiber has been substructured into seven slices. The predicted composite properties/response have been compared to experimental values wherever available, and, although the results are not shown here, composite response/properties are verified with METCAN predictions and detailed three-dimensional finite element analyses.

## Mechanical Properties

Longitudinal and transverse moduli for unidirectional SiC/RBSN composite at three fiber volume ratios 0.2, 0.3, and 0.4 are shown in figures 5 and 6. There is very little degradation in the composite longitudinal modulus with a weak interphase showing that the longitudinal modulus does not depend upon interfacial conditions. The transverse composite modulus shows substantial degradation with a weak interphase showing that the transverse modulus strongly depends upon the matrix properties and the interfacial conditions. Comparison with the experimental values is made in figure 7 for a nominal fiber volume ratio of 0.3. The experimentally measured value for longitudinal modulus is higher than the CEMCAN prediction, but since the longitudinal modulus does not depend upon the interfacial conditions, it suggests that the nominal fiber volume ratio in experimental samples is greater than 0.3. Once, the nominal fiber volume ratio is determined from the measured value of longitudinal composite modulus, one can estimate the interfacial conditions or the amount of debonding a priori by comparing the experimentally measured value of transverse composite modulus and the CEMCAN prediction for that nominal fiber volume ratio. Poisson's ratio $\nu_{12}$ for three different fiber volume ratios and the comparison with the experimental value for 0.3 fvr is shown in figure 8 and the agreement is excellent. Although, the results are not shown here, the METCAN and three-dimensional finite element analyses predictions were in excellent agreement with CEMCAN predictions.

## Thermal Properties

Composite thermal expansion coefficients for the longitudinal and transverse direction for three fiber volume ratios 0.2, 0.3, and 0.4 are shown in figures 9 and 10. The longitudinal thermal expansion coefficient does not depend upon the interfacial debonding as the longitudinal behavior is largely controlled by the fibers, while the transverse thermal expansion coefficient shows substantial increase for a fully debonded interphase as it approaches towards the matrix value. The experimental values for the thermal expansion coefficients at room temperature were not available. The longitudinal and transverse composite thermal conductivities are shown in figure 11 for the same three fiber volume ratios. The only experimental value available was for the longitudinal thermal conductivity at a nominal fvr of 0.3 and is shown in figure 11. The value of thermal conductivity for both strong and weak interphase was taken to be the same, hence the weak or strong interphase does not make a difference on the composite thermal conductivity values. The CEMCAN predictions for the composite thermal expansion coefficients were also compared with METCAN and three-dimensional finite element analyses predictions and they showed excellent agreement.

## Microstresses

Microstresses in all the constituents for both longitudinal and transverse loading are shown in figures 12 and 13, respectively. The microstresses are shown for a unidirectional composite with a fiber volume ratio of 0.3. Since the longitudinal response is largely controlled by the fibers, there is little change in the fiber or matrix stress for longitudinal loading as the interphase is fully debonded. For the transverse loading case, the matrix transverse stress in the A region for the fully debonded interphase becomes approximately three times the stress for the case of strong interphase. If the ratio of the transverse stress to the matrix strength is considered, the matrix in the A region will fail at one-third load for a fully debonded interphase as compared to the case of strong interphase. This suggests that the transverse tensile strength test method can be a sensitive test method to assess interfacial conditions. This is in direct agreement with the authors previous work on composite microfracture (ref. 8). These stress values have been compared to the values predicted by the METCAN computer code and finite element analysis. Although the aggregate, or average values are shown in the figures for a region, the CEMCAN code predicts the stress variation through the ply thickness via fiber substructuring, while the other micromechanics based codes ICAN and METCAN only provide an average value of stress over a region.

### Partial Interphase Bond

The CEMCAN code has a unique feature that allows the user to specify a partial bond around the fiber circumference and then integrate its effect up to composite properties/laminate response. The variation of some mechanical and thermal properties as a function of percent fiber circumference debonded is shown in figure 14. Longitudinal or fiber controlled properties show little degradation, while the transverse properties show greater degradation as a function of debonding. The debonding can also occur due to the oxidation damage to the interphase when the composite is subjected to high temperatures. The degradation of composite properties in a $[0]_5$ composite is shown in figure 15 for different interfacial damage (debonding). If the interfacial damage is limited to only the top and bottom plies (damage 1), there is very little degradation in the composite properties and is difficult to detect by conventional experimental measurements. However, if the experimentally measured values show greater degradation in the composite properties, then the interfacial damage will be more widespread as shown by damage 2 (linearly varying interfacial debonding) or the complete debonding of the interphase in all the plies, as shown by damage 3.

## CONCLUSIONS

A multilevel substructuring technique which involves a unique fiber substructuring concept embedded in the computer code CEMCAN is used to analyze a unidirectional ceramic matrix composite. The formalism in CEMCAN computer code is general and is applicable for the simulation of the behavior in all continuous fiber reinforced composites, although the discussion here is limited to ceramic matrix composites. Based on the results shown, it can be concluded that:

1. Fiber substructuring captures/represents greater local detail than other unit cell based micromechanics theories. Hence, it can simulate aspects unique to ceramic matrix composites such as varying degree of interfacial bonding around the fiber circumference and their effect on composite properties/response.

2. The comparison between CEMCAN predictions and experimentally measured values for a SiC/RBSN composite shows good agreement. The strong and weak interphase represent upper and lower bounds, respectively, for the composite properties.

3. Longitudinal composite properties are independent of interfacial conditions, while the transverse composite properties are strongly influenced by the interfacial conditions.

4. If the interfacial debonding/damage is only limited to a few plies, the degradation in the composite properties is minimal and difficult to detect by conventional experimental measurements.

5. Transverse tensile strength test method can be a sensitive test to assess the interfacial conditions.

6. CEMCAN computer code provides sufficient flexibility to study the interfacial effects and to better interpret the experimental results.

## REFERENCES


1. Chamis, C.C., et al.: METCAN Verification Status. NASA TM–103119, 1990.

2. Lee, H.-J., et al.: METCAN Updates for High Temperature Composite Behavior: Simulation/ Verification. NASA TM–103682, 1991.

3. Murthy, P.L.N., et al.: Second Generation Integrated Composite Analyzer (ICAN) Computer Code. NASA TP–3290, 1993.

4. Lee, H.-J., et al.: Metal Matrix Composite Analyzer (METCAN) User's Manual—Version 4.0. NASA TM–105244, 1991.

5. Murthy, P.L.N.; and Chamis, C.C.: Towards the Development of Micromechanics Equations for Ceramic Matrix Composites via Fiber Substructuring. NASA TM–105246, 1992.

6. Agarwal, B.D.; and Broutman, L.J.: Analysis and Performance of Fiber Composites. Second Edition, Wiley & Sons, New York, 1990.

7. Bhatt, R.T.; and Phillips, R.E.: Laminate Behavior for SiC Fiber-Reinforced Reaction-Bonded Silicon Nitride Matrix Composites. NASA TM–101350, 1988.

8. Mital, S.K.; Chamis, C.C.; and Gotsis, P.K.: Microfracture in High Temperature Metal Matrix Laminates. NASA TM–105189, 1991.


TABLE I.—PROPERTIES OF CONSTITUENT MATERIALS

(SiC/RBSN)

| | SiC fiber | RBSN matrix | Interphase (weak) |
|---|---|---|---|
| Modulus, GPa | 390 | 110 | 0.7 |
| Poisson's ratio | 0.17 | 0.22 | 0.220 |
| Shear modulus, GPa | 150 | 45 | 0.27 |
| Thermal conductivity, w/mK | 1.4 | 15 | 0.7 |
| Thermal expansion coefficient, ppm/C | 2.2 | 23.6 | 8.1 |

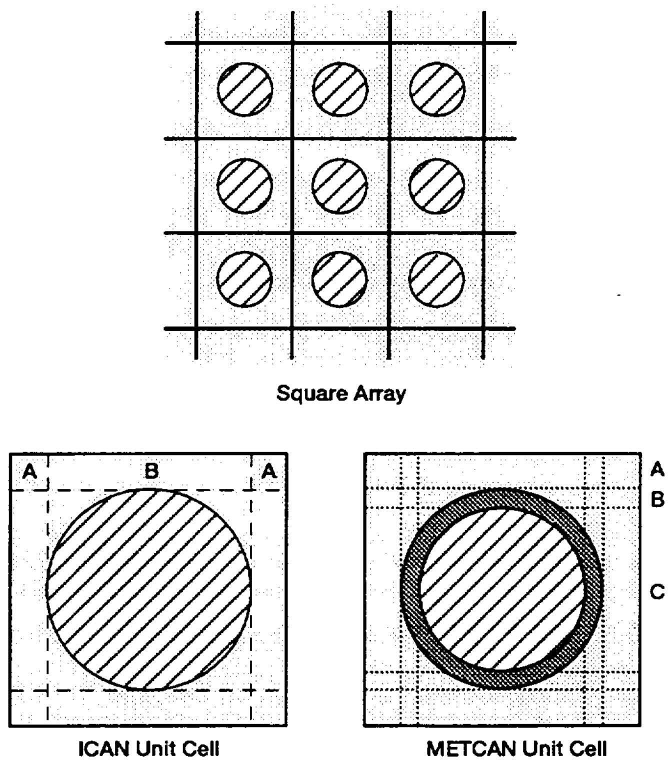


Figure 1.—Unit cell square array concepts in ICAN and METCAN codes.

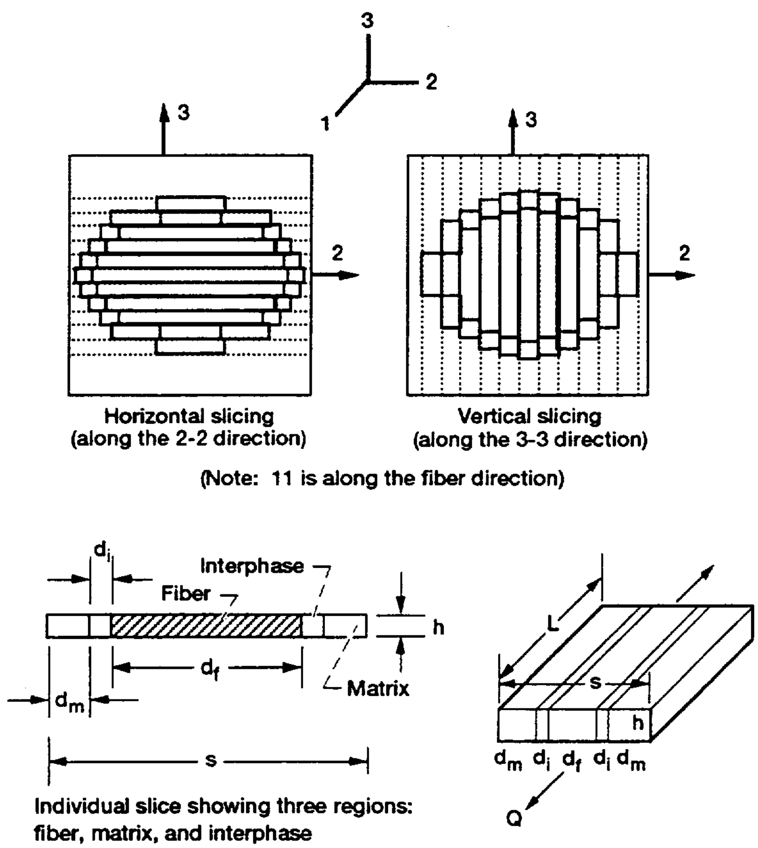


Figure 2.—Ply/fiber substructuring for ceramic matrix composites micromechanics.

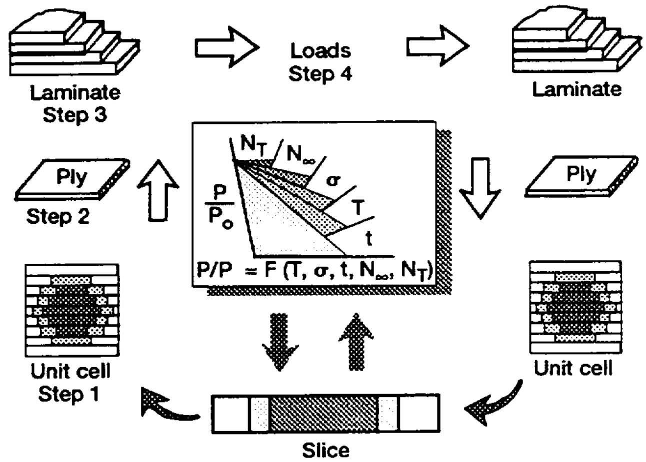

Figure 3.—Integrated analysis approach embedded in CEMCAN.

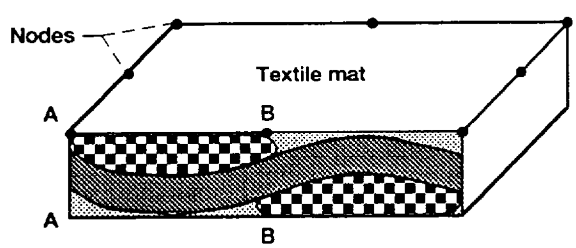

Figure 4.—Typical element of a finite element model of a component made from woven fabric.

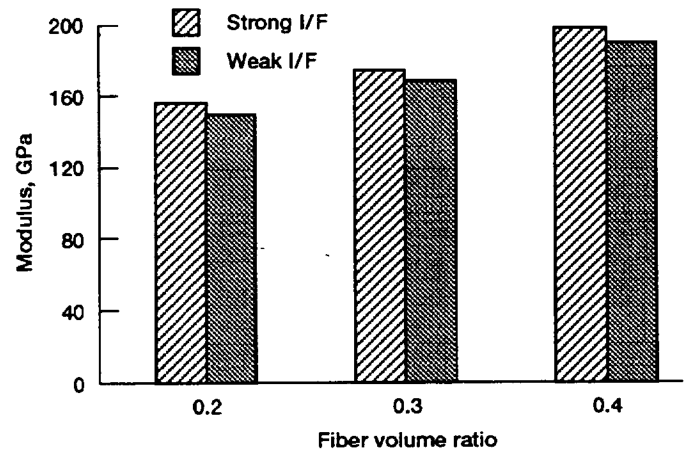

Figure 5.—Longitudinal modulus $E_{\ell 11}$.

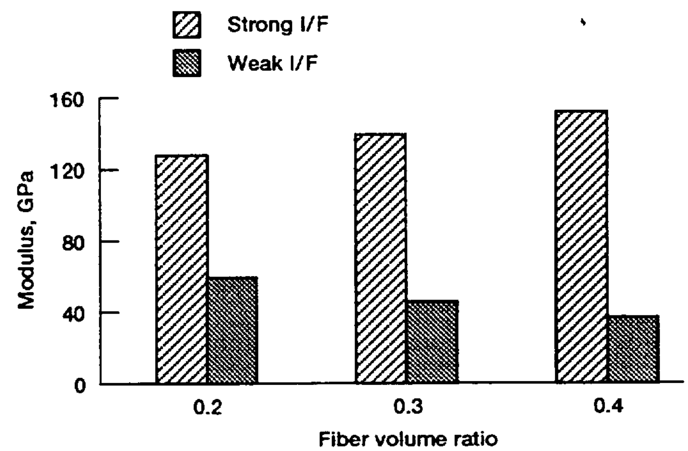

Figure 6.—Transverse modulus $E_{\ell 22}$.

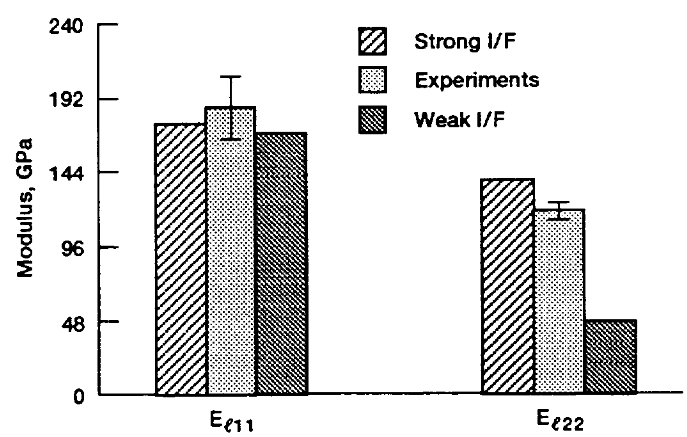

Figure 7.—Prediction of Young's moduli; CEMCAN vs. experiments (fvr 0.3).

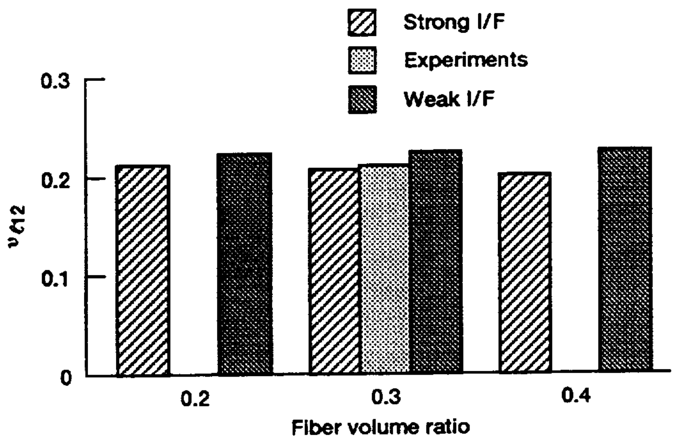


Figure 8.—Poisson's ratio $\nu_{\ell 12}$.

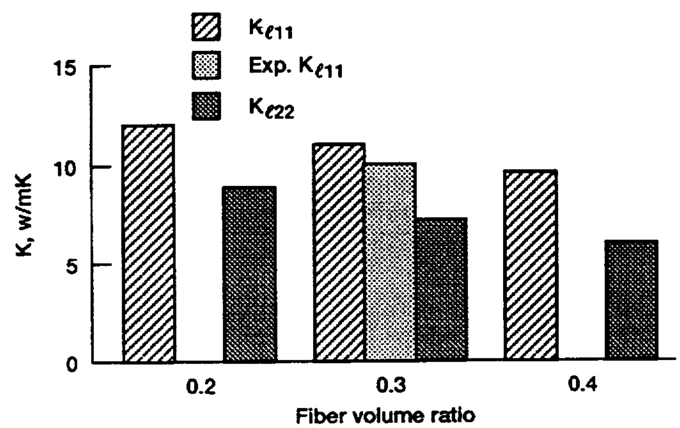


Figure 11.—Longitudinal and transerve thermal conductivities.

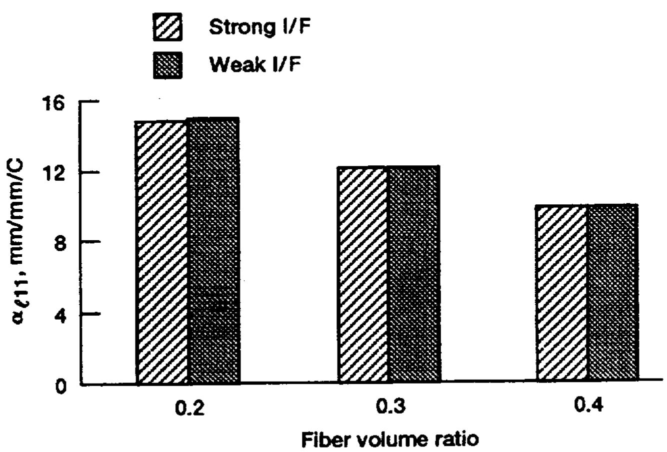


Figure 9.—Longitudinal thermal expansion coefficient $\alpha_{\ell 11}$.

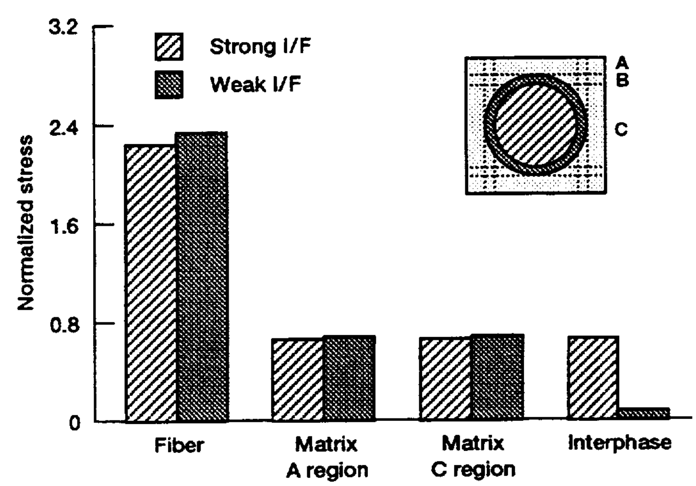


Figure 12.—Longitudinal stress (normalized w.r.t. applied stress) due to the loading in 1-1 direction (fvr 0.3).

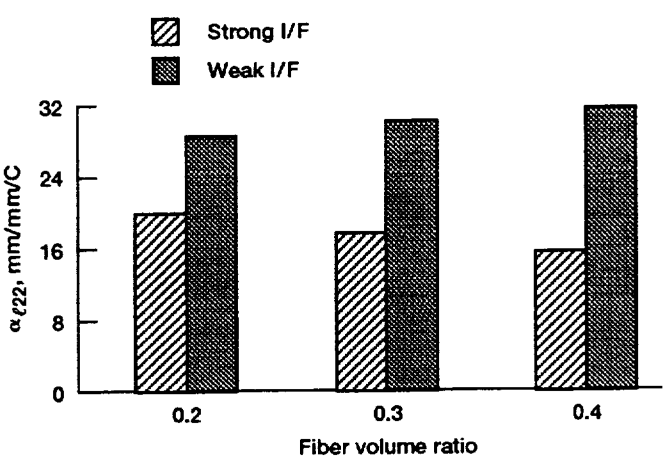


Figure 10.—Transverse thermal expansion coefficient $\alpha_{\ell 22}$.

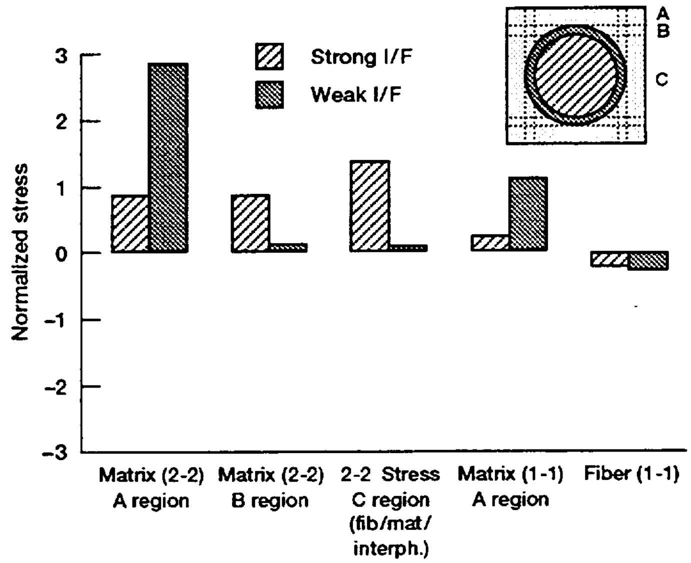


Figure 13.—Microstresses (normalized w.r.t. applied stress) due to loading in 2-2 direction (fvr 0.3).

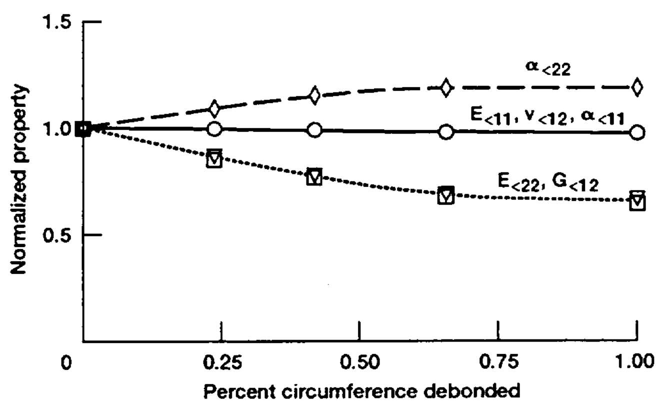


Figure 14.—Variation of thermal and mechanical properties (normalized w.r.t. property with strong interphase) due to partial bonding (fvr 0.3).

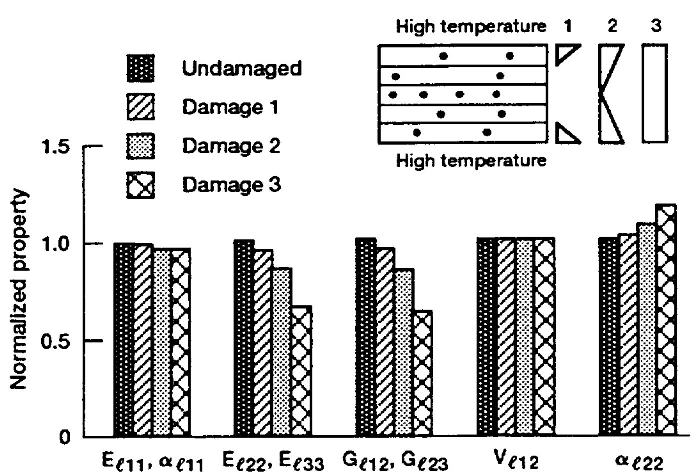


Figure 15.—Comparison of composite properties (normalized w.r.t. property with undamaged interphase) due to interfacial damage through the thickness (fvr 0.3).

# REPORT DOCUMENTATION PAGE

Form Approved
OMB No. 0704-0188



**1. AGENCY USE ONLY** *(Leave blank)*

**2. REPORT DATE**
May 1993

**3. REPORT TYPE AND DATES COVERED**
Technical Memorandum

**4. TITLE AND SUBTITLE**
Ceramic Matrix Composites Properties/Microstresses With Complete and Partial Interphase Bond

**5. FUNDING NUMBERS**
WU-510-01-50

**6. AUTHOR(S)**
S.K. Mital, P.L.N. Murthy, and C.C. Chamis

**7. PERFORMING ORGANIZATION NAME(S) AND ADDRESS(ES)**
National Aeronautics and Space Administration
Lewis Research Center
Cleveland, Ohio 44135–3191

**8. PERFORMING ORGANIZATION REPORT NUMBER**
E–7816

**9. SPONSORING/MONITORING AGENCY NAME(S) AND ADDRESS(ES)**
National Aeronautics and Space Administration
Washington, D.C. 20546–0001

**10. SPONSORING/MONITORING AGENCY REPORT NUMBER**
NASA TM–106136

**11. SUPPLEMENTARY NOTES**
Prepared for the 38th International SAMPE Symposium/Exhibition, Anaheim, California, May 10–13, 1993. S.K. Mital, University of Toledo, Toledo, Ohio 43606 and P.L.N. Murthy and C.C. Chamis, NASA Lewis Research Center. Responsible person, C.C. Chamis, (216) 433–3252.

**12a. DISTRIBUTION/AVAILABILITY STATEMENT**
Unclassified - Unlimited
Subject Category 24

**12b. DISTRIBUTION CODE**

**13. ABSTRACT** ***(Maximum 200 words)***

A multilevel substructuring technique which includes a unique fiber substructuring concept is used for the analysis of continuous fiber reinforced ceramic matrix composites. This technique has four levels of substructuring – from laminate to ply, to subply, and then to fiber. A stand-alone computer code CEMCAN (CEramic Matrix Composites ANalyzer), incorporating this technique and specifically for the simulation of ceramic matrix composites behavior, is currently under development at NASA Lewis Research Center in Cleveland, Ohio. The thermal and mechanical properties, along with the microstresses, for a SiC/RBSN (silicon carbide fiber and reaction bonded silicon nitride matrix) composite at different fiber volume ratios and varying degrees of interfacial bond around the fiber circumference are computed. Values predicted by CEMCAN computer code are shown to bound the experimentally measured values. Results also show that transverse tensile strength test can be a sensitive test method to assess interfacial conditions.

**14. SUBJECT TERMS**
Thermal properties; Mechanical properties; Computational simulation; Micromechanics equations; Macromechanics; RBSN matrix; Resident databank; Fiber substructuring; Unit cell; Interphase

**15. NUMBER OF PAGES**
12

**16. PRICE CODE**
A03

| 17. SECURITY CLASSIFICATION OF REPORT | 18. SECURITY CLASSIFICATION OF THIS PAGE | 19. SECURITY CLASSIFICATION OF ABSTRACT | 20. LIMITATION OF ABSTRACT |
|---|---|---|---|
| Unclassified | Unclassified | Unclassified | |